Title:

Intra- and Inter-Specific Investigations of Skeletal DNA Methylation Patterns and Femur Morphology in Nonhuman Primates

Authors and Affiliations:

Genevieve Housman[1,2*], Ellen E. Quillen[3], and Anne C. Stone[1,2]

[1]School of Human Evolution and Social Change, Arizona State University, Tempe, AZ, USA.
[2]Center for Evolution and Medicine, Arizona State University, Tempe, AZ, USA.
[3]Department of Genetics, Texas Biomedical Research Institute, San Antonio, TX, USA.

*Corresponding author:
Genevieve Housman, Section of Genetic Medicine, University of Chicago, 920 East 58th Street, CLSC 317, Chicago, IL 60637, USA. Email: ghousman@uchicago.edu

Author Notes:

Genevieve Housman is currently affiliated with the University of Chicago, and Ellen E. Quillen is currently affiliated with Wake Forest School of Medicine.

Key Words: DNA methylation, nonhuman primates, evolution, epigenome, bone

Abstract:

Epigenetic mechanisms influence the development and maintenance of complex phenotypes and may also contribute to the evolution of species-specific phenotypes. With respect to skeletal traits, little is known about the gene regulation underlying these hard tissues or how tissue-specific patterns are associated with bone morphology or vary among species. To begin exploring these topics, this study evaluates one epigenetic mechanism, DNA methylation, in skeletal tissues from five nonhuman primate species which display anatomical and locomotor differences representative of their phylogenetic groups. First, we test whether intra-specific variation in skeletal DNA methylation is associated with intra-specific variation in femur morphology. Second, we identify inter-specific differences in DNA methylation and assess whether these lineage-specific patterns may have contributed to species-specific morphologies. Specifically, we use the Illumina Infinium MethylationEPIC BeadChip to identify DNA methylation patterns in femur trabecular bone from baboons (n=28), macaques (n=10), vervets (n=10), chimpanzees (n=4), and marmosets (n=6). Significant differentially methylated positions (DMPs) were associated with a subset of morphological variants, but these likely have small biological effects and may be confounded by other variables associated with morphological variation. Conversely, several species-specific DMPs were identified, and these are found in genes enriched for functions associated with complex skeletal traits. Overall, these findings reveal that while intra-specific epigenetic variation is not readily associated with skeletal morphology differences, some inter-specific epigenetic differences in skeletal tissues exist and may contribute to evolutionarily distinct phenotypes.

Introduction:

Primates distinguish themselves from other mammals with their unique suite of anatomical features that initially enabled arboreal niche occupation and subsequently evolved to fit a myriad of habitats and forms of locomotion, the most unique being hominin bipedalism. The resulting morphological variation that has evolved across taxa has its foundation in underlying skeletal anatomies. Such skeletal morphologies are used to both characterize extant primate diversity and reconstruct the anatomy and locomotor capabilities of extinct primate species (Schultz 1930; Schultz 1937; Leigh and Shea 1995; Fleagle 1999; Ankel-Simons 2007). The range of mechanisms that enable the development of skeletal features are not entirely understood, though. Skeletal features related to varied body forms are often described as the result of environmental adaptations. However, skeletal morphology is more accurately defined as the result of complex processes, including environmental, genetic, and epigenetic mechanisms. While environmental (Henriksen et al. 2014; Lewton 2017; Lewton et al. 2018; Macrini et al. 2013) and genetic (Smith et al. 2014; Joganic et al. 2017; Ritzman et al. 2017) factors have been readily explored, the important roles of epigenetic factors, such as DNA methylation, in skeletal tissue development and maintenance have only recently been identified (Delgado-Calle et al. 2013; Goldring and Marcu 2012; García-Ibarbia et al. 2013; Liu et al. 2013; Loughlin and Reynard 2015; Ostanek et al. 2018; Ramos et al. 2014; Reynard et al. 2014; Reynard 2017; Simon and Jeffries 2017).

For instance, epigenetic processes are influential in regulating skeletal muscle development (Brand-Saberi 2005; Palacios and Puri 2006; Pandorf et al. 2009; Zwetsloot et al. 2009; Ling et al. 2012) which can impact the adjacent skeletal scaffolding system. Several genes involved in human skeletal development appear to be differentially methylated across fetal and adult developmental stages (de Andrés et al. 2013). Lastly, methylation variation in humans and

model organisms has been implicated in several skeletal pathologies and disorders, such as rheumatoid arthritis, osteoporosis, and osteoarthritis (Iliopoulos et al. 2008; Rivadeneira et al. 2009; Bovée et al. 2010; Ralston and Uitterlinden 2010; Dimitriou et al. 2011; Goldring and Marcu 2012; Delgado-Calle et al. 2013; García-Ibarbia et al. 2013; Kasaai et al. 2013; Liu et al. 2013; Fernández-Tajes et al. 2014; den Hollander et al. 2014; Jeffries et al. 2014; Moazedi-Fuerst et al. 2014; Ramos et al. 2014; Reynard et al. 2014; Rushton et al. 2014; Loughlin and Reynard 2015; Jeffries et al. 2016; Morris et al. 2017; Reynard 2017). Some of these studies are the first to assess methylation patterns in human skeletal tissues (Delgado-Calle et al. 2013; García-Ibarbia et al. 2013; Fernández-Tajes et al. 2014; den Hollander et al. 2014; Jeffries et al. 2014; Moazedi-Fuerst et al. 2014; Rushton et al. 2014), and such steps are important for truly identifying the relationship between epigenetic variation and skeletal phenotypic variation.

The contributions of epigenetics to primate phenotypic variation were first considered by King and Wilson (1975), who proposed that anatomical and behavioral differences between humans and chimpanzees were more likely "based on changes in the mechanisms controlling the expression of genes than on sequence changes in proteins" (King and Wilson 1975). Studies to understand methylation variation across species began soon afterwards (Gama-Sosa et al. 1983). General changes to mammalian epigenomes have been examined (Sharif et al. 2010), but most epigenetics work in primates has focused on humans – how it varies across distinct tissues within individuals (Lister et al. 2009; Slieker et al. 2013), across different individuals (Weksberg et al. 2002; Petronis et al. 2003; Oates et al. 2006), across populations (Rakyan et al. 2004; Heyn et al. 2013), in relation to aging processes (Fraga et al. 2005), and in relation to diet (Jacob et al. 1998; Rampersaud et al. 2000; Shelnutt et al. 2004), as well as how it is inherited across generations (Suter et al. 2004; Flanagan et al. 2006; Gibbs et al. 2010; van Dongen et al. 2014). These studies have identified important within species methylation variants.

Similarly, epigenetic variation has been identified among primate species. Inter-specific variation in epigenetic signatures was initially inferred from underlying genomic sequences (Haygood et al. 2007; Prendergast et al. 2007; Bell et al. 2012). For instance, several promoter CpG densities vary across primates. These likely relate to regulatory methylation differences across species as primate CpG densities correlate with methylation levels (Weber et al. 2007). Additionally, gene expression studies, which primarily focus on brain tissues (Cáceres et al. 2003; Warner et al. 2009; Babbitt et al. 2010) and a small set of other soft tissues (Blekhman et al. 2008; Karere et al. 2010; Karere et al. 2012; Karere et al. 2013; Tung et al. 2015), have also noted regulatory differences across species. Methylation differences in brain tissues have evolved across primates and contributed to resultant brain phenotypes and disease vulnerabilities (Enard et al. 2004; Kothapalli et al. 2007; Farcas et al. 2009; Provencal et al. 2012; Zeng et al. 2012; Mendizabal et al. 2016; Madrid et al. 2018). Thus, methylation-phenotype relationships can be identified in primates. Primate methylation patterns in blood cells and other soft tissues have also been studied, but not to the same degree (Martin et al. 2011; Molaro et al. 2011; Pai et al. 2011; Fukuda et al. 2013; Hernando-Herraez et al. 2013; Lindskog et al. 2014; Lea et al. 2016; Gao et al. 2017; Vilgalys et al. 2018).

Interestingly, two studies using soft tissues and blood identified differential methylation and expression of genes essential for skeletal development (*RUNX1*, *RUNX3*, and *COL2A1*) between some primates (Hernando-Herraez et al. 2013; Lindskog et al. 2014). Additionally, the emerging field of ancient epigenetics, which reconstructs methylation patterns from ancient DNA degradation patterns in hominin remains (Smith et al. 2015; Gokhman et al. 2014; Gokhman et al. 2016; Gokhman et al. 2017), have found that other skeletal developmental genes

(*HOXD* complex) are differentially methylated among modern humans and ancient hominins (Gokhman et al. 2014). These findings suggest that primates do exhibit distinct epigenetic patterns and that the epigenetics of skeletal development may be an important area of research. Nevertheless, studies of nonhuman primate (NHP) skeletal epigenetics are limited (Housman et al. 2018).

Overall, there are clear knowledge gaps in our understanding of NHP skeletal complexity in relation to epigenetic variation and epigenetic differences between phylogenetically diverse NHP species. The present study begins to remedy this by assessing how genome-wide and gene-specific DNA methylation in primate skeletal tissues varies intra- and inter-specifically and in relation to femur form. Specifically, for this study, we explored the evolution of the epigenome and its relation to nonpathological skeletal traits by identifying DNA methylation patterns in femur trabecular bone from baboons, macaques, vervets, chimpanzees, and marmosets and assessing intra- and inter-specific methylation variation and its relation to morphology.

Results:

The aim of this study was to identify DNA methylation patterns in skeletal tissues from several NHP species in order to determine how skeletal methylation varies at different taxonomic scales and in relation to complex skeletal traits. We evaluated DNA methylation patterns in femur trabecular bone from five NHP species – baboons (n=28), macaques (n=10), vervets (n=10), chimpanzees (n=4), and marmosets (n=6) (Figure 1, Table S1). We used the Illumina Infinium MethylationEPIC BeadChip (EPIC array), which was determined to be effective at identifying DNA methylation patterns in NHP DNA (Supplemental Text, Figures S1-S4, Tables S2-S5, File S1). Further, we selected probes appropriate for intra- and inter-specific comparison, which removed the effect of sequence differences among individuals and species as a reason for methylation differences. With these data, we first tested whether intra-specific variation in skeletal DNA methylation is associated with intra-specific variation in femur morphology. Second, we identified inter-specific differences in DNA methylation and assessed whether these lineage-specific patterns may have contributed to species-specific morphologies.

Genome-Wide Intra-Specific Differential Methylation and Morphological Variation

Measurements of 29 linear morphology traits (Figure 2, Table S6) were collected from each NHP right femur. All measurements had less than 5% error, except those for intercondylar notch depth in macaques (Figure S5, File S2). Significant differentially methylated positions (DMPs) associated with each intra-specific linear morphology were interrogated from 189,858 sites in in baboons, 190,898 sites in macaques, 191,639 sites in vervets, 576,804 sites in chimpanzees, and 68,709 sites in marmosets (Tables S7-S8). In baboons, 1 DMP was hypomethylated with increasing bicondylar femur length and increasing maximum femur length. In macaques, 1 DMP was hypermethylated with increasing proximal femur width, 1 DMP was hypermethylated with increasing medial condyle width, and 6 DMPs were hypomethylated with increasing medial condyle width. In vervets, 1 DMP was hypomethylated with increasing superior shaft width, 2 DMPs were hypomethylated with increasing inferior shaft width, and 1 DMP was hypermethylated with increasing anatomical neck height. In chimpanzees, 216 DMPs were hypomethylated and 57 DMPs were hypermethylated with increasing anatomical neck length. Lastly, in marmosets, no DMPs were associated with morphological variation (Table S9, File S3).

While the maximum change in mean methylation (Δβ) for most of these DMPs is greater than 10% (Δβ = 0.1), the actual Δβ between individuals with the largest morphology measurements and individuals with the smallest morphology measurements is less than 0.1 for several DMPs (File S3). Tests for enrichment of gene ontology (GO) and KEGG pathway functions were done for the 3 intra-specific morphologies that had more than 2 DMPs associated with them. However, no GO biological processes were found to be enriched in DMPs associated with either macaque medial condyle width or chimpanzee anatomical neck length. Additionally, KEGG pathway functions were only found to be enriched in DMPs associated with chimpanzee anatomical neck length, and these pathways were predominantly involved in immune system cell signaling and differentiation (Table S10).

Genome-Wide Inter-Specific Differential Methylation

To determine how methylation varies inter-specifically, differential methylation was interrogated from the 39,802 probes that were shared among NHP species (Table S11, File S4). Species-specific DMPs were determined by identifying DMPs that were significant in all 4 pairwise comparisons containing the taxon of interest but not in any of the remaining pairwise comparisons. These methods identified 650 species-specific DMPs in baboons, 257 in macaques, 639 in vervets, 2,796 in chimpanzees, and 13,778 in marmosets (Table S11). Comparably, when evaluating methylation patterns that distinguish more broad taxonomic groups, 2,701 DMPs were found to be specific to Old World monkeys (OWMs), 1,439 were found to be ape-specific, and 15,514 were found to be specific to New World monkeys (NWMs) (File S5). Species-specific DMPs spanned 7,320 genes (Table S12). While 4,824 of these genes have only a single probe targeting them, the remaining 2,496 genes contained at least 2 significant probes. Additionally, these species-specific DMPs covered a range of locations with respect to genes and CpG islands (Table S12), indicating that these species-specific changes in methylation have a decent distribution throughout the genome. Using various Δβ cutoff thresholds decreases the final number of species-specific DMPs to varying degrees (Table S11, File S4). Counter to these decreases in numbers, though, species-specific DMPs cover a range of locations with respect to genes and CpG islands regardless of the Δβ cutoff threshold (Table S12).

Overall, across Δβ cutoff thresholds, more species-specific DMPs were found in the NWM marmosets, followed by the great ape chimpanzees, and lastly the OWM baboons, macaques, and vervets. Additionally, the proportions of hypermethylated and hypomethylated species-specific DMPs within each taxon remain fairly constant across Δβ cutoff thresholds (Table S11). In baboons, macaques, vervets, and chimpanzees, more than half of all species-specific DMPs show patterns of hypermethylation, and in marmosets, more than half of all species-specific DMPs show patterns of hypomethylation. The only disruption in these trends is in chimpanzees when no Δβ threshold is applied. Nevertheless, species-specific DMPs with different Δβ cutoff thresholds do differ in their abilities to cluster animals into taxonomic groups (Figure S6, File S4). For all thresholds, apes, OWMs, and NWMs cluster into distinct groups. However, within OWMs, vervets only cluster into a distinct species group with a $\Delta\beta \geq 0.2$ threshold, and the baboon-macaque clade require a $\Delta\beta \geq 0.3$ threshold. Lastly, species-specific clustering of baboons, macaques, and vervets only occurs with a $\Delta\beta \geq 0.4$ threshold (Figure 3).

Additionally, global changes in methylation across all 39,802 probes were evaluated. Average global changes within each species reveal that apes, OWMs, and NWMs are phylogenetically distinct from one another, and these divergences are well supported (Figure 4). Similarly, when phylogenetic relationships are evaluated using the global changes in methylation

of individual animals, distinct lineages are again formed between apes, OWMs, and NWMs (Figure S7). However, within the OWM clade, several poorly supported branches result in baboons, macaques, and vervets not forming distinct lineages. Phylogenetic separation of these OWM species into distinct lineages is only possible when the methylation changes considered are reduced to only include species-specific DMPs with a $\Delta\beta \geq 0.4$ threshold (Figure S8).

Species-specific DMPs also show associations with genes that have a wide array of GO biological processes (File S6) and KEGG pathway functions (File S7). Cellular adhesion is a primary GO function found to be highly enriched in species-specific DMPs from macaques, vervets, chimpanzees, and marmosets. Species-specific DMPs for chimpanzees and marmosets are also enriched for genes involved in the regulation of transcription and gene expression. Additionally, enrichment of genes involved in anatomical developmental processes is found in baboons, chimpanzees, and marmosets. Chimpanzees and marmosets show further enrichment of genes contributing to pattern specification processes, limb development, and skeletal system development. Moreover, marmoset species-specific DMPs are enriched for genes with functions very closely related to skeletal development, such as osteoblast differentiation and ossification, as well as genes involved in metabolism and the development of other organ systems including skeletal muscles, nerves, the brain, the heart, blood vessels, kidneys, eyes, and ears (File S6). Several enriched pathways reinforce these molecular functions, and additional pathways related to cancers and other disease were also identified (File S7).

Out of the species-specific DMPs identified, some were found to overlap with those previously identified as being differentially methylated among primates. These include *ARTN*, *COL2A1*, and *GABBR1* which have been found to be differentially methylated among modern humans and great apes (Hernando-Herraez et al. 2013), as well as *HOXD8*, *HOXD9*, and *HOXD10* which have been found to be differentially methylated among modern and ancient hominins (Gokhman et al. 2014). Specifically, 1 marmoset-specific DMP is hypomethylated in *ARTN*, 3 marmoset-specific DMPs are hypermethylated in *COL2A1*, 2 baboon-specific DMPs and 3 marmoset-specific DMPs are hypermethylated in *GABBR1*, and 2 marmoset-specific DMPs are hypomethylated in *GABBR1* (File S4). Additionally, 3 marmoset-specific DMPs are hypermethylated in *HOXD8*, 1 baboon-specific DMP and 2 marmoset-specific DMPs are hypermethylated in *HOXD9*, 2 chimpanzee-specific DMPs are hypomethylated in *HOXD9*, and 5 marmoset-specific DMPs are hypermethylated in *HOXD10*. Of these *HOXD10* species-specific DMPs, 4 have $\Delta\beta$ between 0.2 and 0.3 and 1 has a $\Delta\beta < 0.1$ (Figure 5, Table S13).

Gene-Specific Inter-Specific DNA Methylation Profiling

Because of the high number of species-specific DMPs within *HOXD10*, methylation patterns across this gene were assessed at a higher resolution using gene-specific sequencing techniques. Regular and bisulfite sequences of several regions in the *HOXD10* gene were generated (Tables S14-S17). First, loci across the entire *HOXD10* gene were examined from a subset of EPIC array samples – 3 baboons, 3 macaques, 3 vervets, 3 chimpanzees, and 3 marmosets (Figure 6, Tables S1 and S18, File S8-S9). Additionally, one validation locus (cg02193236) and its surrounding region in *HOXD10* were surveyed in all NHP samples in order to confirm the reliability of the EPIC array in assessing DNA methylation levels (Figure S9, Tables S1 and S19, File S10-S11). Overall, regular sequencing was very successful, while bisulfite sequencing was less successful, with several sequence reads uninterpretable. Nevertheless, following the alignment of these sequences to the appropriate NHP references, the presence and absence of methylation across the *HOXD10* gene in each animal was determined

(Tables S18-S19, Files S8-S11). These data reveal that across the *HOXD10* gene, NHPs display generally low methylation with some clustered increased amounts of methylation upstream of the gene and at the start of the gene body (Figure 6).

Discussion:

This study explored skeletal gene regulation and its relation to complex traits and species differences by evaluating genome-wide and gene-specific DNA methylation patterns in trabecular bone from several NHP species. These species are phylogenetically representative of the order and display anatomical and locomotor differences. Specifically, while the sampled OWMs (baboons, macaques, vervets) display varying levels of terrestrial and arboreal quadrupedal locomotion, the sampled ape species (chimpanzees) is a knuckle-walking quadruped that also vertical climbs and occasionally walks bipedally (Cawthon Lang 2006). Even more distinct are the sampled NWMs (marmosets) which locomote via vertical clinging and leaping (Cawthon Lang 2005). Lemurs and lorises are the only major taxonomic primate groups not examined in this study. Regardless, the current sample set provided a unique opportunity to examine skeletal epigenetic differences in relation to bone morphology. First, we evaluated the association between intra-specific variation in skeletal DNA methylation and intra-specific variation in femur morphology. Second, we assessed inter-specific DNA methylation differences and the potential contribution of these lineage-specific patterns to species-specific morphologies.

Intra-specific DMPs are not readily associated with morphological variants.

With respect to intra-specific morphology, very few sites were found to be differentially methylated. DMPs were only identified in association with baboon bicondylar femur length, baboon maximum femur length, macaque proximal femur width, macaque medial condyle width, vervet superior shaft width, vervet inferior shaft width, vervet anatomical neck height, and chimpanzee anatomical neck length (Table S8). Additionally, most of these associations only identified one DMP. This limited number of associations may be due to the small sample sizes within each species or to the small amount of variation identified in each morphology. This latter point is supported in that almost all the morphologies with methylation associations also have the highest intra-specific variation in size (Figure S5, Files S2-S3). Further, because the animals included in this study were born and raised in captivity, their limited exposure to environmental variation may limit both the range of phenotypic variation and methylation variation present within species. Alternatively, it may be the case that DNA methylation variation does not have a large influence on nonpathological femur morphology within NHPs.

Of the few intra-specific methylation patterns associated with morphology, they likely have weak functional effects. Research has shown that individual site-specific methylation changes are not readily associated with differential gene expression (Bork et al. 2010; Chen et al. 2011; Koch et al. 2011). Rather, differential gene expression is made possible through the accumulation of several methylation changes within promotor regions (Suzuki and Bird 2008) or across the gene body (Singer et al. 2015). Detecting accumulations of methylation changes across genes should have been possible in the current study as 4-19 probes targeted each gene on average (Table S4). Thus, the individual sites identified in this study are not due to experimental limitations and likely have limited impacts on gene regulation. This is further supported by the degree of methylation variation observed among these DMPs. Sites that have an average change in mean methylation less than 10% ($\Delta\beta < 0.1$) are thought to have little biological relevance (Hernando-Herraez et al. 2013). Thus, those DMPs with small changes in methylation likely

have little to no biological function. Further, some of the DMPs with $\Delta\beta \geq 0.1$ appear to be highly influenced by small subsets of the sample sets. For example, in the case of macaque proximal width, the majority of methylation change is due to two individuals (1 female and 1 male) that have extremely low methylation at cg19349877 as compared to other macaques (File S3). Additionally, in the case of chimpanzee anatomical neck length, the 273 DMPs identified are largely affected by one individual that has a longer anatomical neck than other chimpanzees. Lastly, the limited enrichment of GO biological processes and KEGG pathway functions among detected DMPs indicates a lack of common function among these associated regions. Overall, these finding suggest that while some DMPs appear to be associated with intra-specific morphological variation in NHPs, not enough evidence is present to support them having a functional role in the development and maintenance of this morphological variation.

Differential methylation is observed among NHP species.

With respect to inter-specific variation, several sites were found to have significant species-specific methylation differences. Specifically, out of the 39,802 sites examined, 650 species-specific DMPs were identified in baboons, 257 in macaques, 639 in vervets, 2,796 in chimpanzees, and 13,778 in marmosets, and these span 7,320 genes (Tables S11-S12). However, many of these DMPs had biologically insignificant changes in mean methylation. Thus, several $\Delta\beta$ cutoff thresholds were considered – from a 10% change in mean methylation ($\Delta\beta \geq 0.1$) up to a 40% change in mean methylation ($\Delta\beta \geq 0.4$) – which reduced the overall numbers of species-specific DMPs. Regardless of $\Delta\beta$ cutoff threshold, more species-specific DMPs were found in the NWM marmosets, followed by the great ape chimpanzees, and lastly the OWM baboons, macaques, and vervets. This trend in numbers of species-specific DMPs is expected given the known phylogenetic relationships between primates, with OWMs more closely related to apes and NWMs more distantly related to both groups (Perelman et al. 2011; Rogers and Gibbs 2014). However, the number of marmoset-specific DMPs is substantially larger than those for other taxa. While this discrepancy may reflect marmosets having more species-specific changes, aspects of the experimental design may also contribute to it. Marmosets are the only NWM included in this study, so although some marmoset-specific DMPs are truly specific to marmosets, others may be specific to all NWMs. Comparably, OWM-specific DMPs and catarrhine-specific DMPs may be cancelled out from this study, as such changes would be shared between all OWMs and catarrhines, respectively. Second, since marmosets are the most phylogenetically distant from humans as compared to the other NHPs included in this study (Perelman et al. 2011; Rogers and Gibbs 2014), the probe filtering steps may have biased downstream data in favor of finding significant results primarily in marmosets. Third, the marmoset data itself has a slightly different normalized distribution, with more mean methylation levels of 50%, than that for other NHPs (Figure S4), which may be due to the chimerism often observed in marmosets. Although, computationally, the filtered array probes examined in this study appear to hybridize sufficiently for marmosets (Figure S3), there may be other unknown biological or technical issues that impede proper DNA methylation analyses from the EPIC array in marmosets and may have inflated the overall number of marmoset-specific DMPs identified.

The number of species-specific DMPs identified in this study, is comparable to those identified in a previous study that assessed methylation patterns in blood from chimpanzees, bonobos, gorillas, and orangutans using the 450K array and similar alignment criteria filtering methods with a focus on sites that had a $\Delta\beta \geq 0.1$ (Hernando-Herraez et al. 2013). This research used a final set of 99,919 probes that were shared across all great ape species and covered 12,593

342 genes with at least 2 probes per gene. Out of these, 2,284 species-specific DMPs were found in
343 humans, 1,245 in chimpanzees and bonobos, 1,374 in gorillas, and 5,501 in orangutans
344 (Hernando-Herraez et al. 2013). In the current study, when a $\Delta\beta \geq 0.1$ threshold was used, only
345 1,572 chimpanzee-specific DMPs were identified (Table S11). This number is lower than the
346 number found in previous research comparing chimpanzees to other great apes (Hernando-
347 Herraez et al. 2013), species that are evolutionarily closer to chimpanzees than are OWMs and
348 NWMs (Perelman et al. 2011; Rogers and Gibbs 2014). However, the total number of sites
349 examined in the present study is approximately one-third of that examined in the prior great ape
350 study. Thus, a 3-fold increase in the number of sites examined might identify a 3-fold increase in
351 chimpanzee-specific DMPs as compared to OWMs and NWMs, which would be closer to
352 expectations (Hernando-Herraez et al. 2013).
353 Additionally, the number of DMPs that distinguish species from one another in the
354 current study is substantially smaller than the numbers of DMPs identified between different
355 skeletal tissue types, between different age cohorts, and between individuals with different
356 skeletal disease states within a NHP species (Housman et al. 2018). This finding is to be
357 expected since differences in DNA methylation which regulate gene expression (Suzuki and Bird
358 2008; Singer et al. 2015) should increase or decrease with the degree of differences between
359 cellular functions among comparative groups (Zhang et al. 2013). In the case of different tissues,
360 substantial DNA methylation differences likely promote distinct gene regulation that is necessary
361 for cells in different tissues to promote different functions. In the case of different age cohorts,
362 slightly fewer DNA methylation differences within the same skeletal tissue may allow cells to
363 emphasize efforts on growth and development in juveniles, as compared to maintenance in
364 adults, without altering the general skeletal-related functions of this tissue. In the case of
365 osteoarthritic disease states, even fewer regulatory changes may be needed to initiate the
366 dysregulation of tissue function. Finally, the comparatively small number of DNA methylation
367 differences between adult, skeletally healthy, NHP species seems reasonable given that other
368 studies have also noted the presence of more regulatory variation within species than between
369 species (Uebbing et al. 2016). In summary, epigenetic and regulatory differences, which control
370 and enable age-dependent organ functions, should be greater within a species when comparing
371 between tissue types, age cohorts, and disease states, than when comparing between species.
372 When evaluating how well the methylation patterns at species-specific DMPs cluster
373 samples, a $\Delta\beta \geq 0.4$ threshold is necessary to achieve clustering into distinct species (Figure 3).
374 Less stringent $\Delta\beta$ thresholds are able to separate apes, NWMs, and OWMs into distinct groups,
375 but the OWMs do not form monophyletic species groups at these thresholds (Figure S6). Global
376 changes in methylation show similar phylogenetic patterns. While average species methylation
377 patterns reveal a well-supported tree topology that reflects known phylogenetic relationships
378 between taxa (Perelman et al. 2011; Rogers and Gibbs 2014) (Figure 4), global changes in
379 methylation among individual animals do not distinguish OWMs into distinct monophyletic
380 groups (Figure S7). As before, parsing down these global changes to only species-specific DMPs
381 with $\Delta\beta \geq 0.4$ fixes the phylogeny (Figure S8). In previous studies, global methylation changes
382 were able to separate great apes into species-specific phylogenetic groups (Hernando-Herraez et
383 al. 2013). Conversely, the need for a higher $\Delta\beta$ cutoff threshold to distinguish species in the
384 current study may be due to evolutionary reasons.
385 The divergence times between OWMs (baboons, macaques, and vervets) are comparable
386 to those between great apes (humans, chimpanzees, gorillas, and orangutans) (Perelman et al.
387 2011). Thus, divergence times do not explain why global changes in methylation are unable to

resolve species-specific phylogenetic clades in the current study as compared to previous research. On the other hand, while nonhuman great apes have experienced higher rates of molecular evolution as compared to humans (Elango et al. 2006), baboons and macaques have slow rates of molecular evolution as compared to other OWMs (Elango et al. 2009), which may correspond to slower rates of epigenetic evolution. This might make baboons and macaques appear more similar to vervets than expected, and further, this may make resolving the phylogenetic divergences between OWMs more difficult than that between the great apes. Additionally, the number of sites included in the present study (39,802) as compared to previous studies (99,919) (Hernando-Herraez et al. 2013) may limit the ability of the present study to fully resolve species-specific lineages. This is reinforced by the low support of several branches in the phylogeny based on global changes in methylation across individual animals (Figure S7). Conversely, sample size was likely not a contributing factor to the discrepancies between the current study (n=58) and previous studies (n=32) (Hernando-Herraez et al. 2013), as the current study has a slightly larger sample size. However, the number of individuals per species was more uniform in previous studies (Hernando-Herraez et al. 2013) than in the current study.

Alternatively, the fact that global changes in methylation are unable to fully resolve OWM species-specific phylogenetic clades in the current study, may instead indicate that not enough time has passed for OWM species to evolve fixed epigenetic changes between taxa in this tissue. Additionally, it is possible that epigenetic variation at many of the sites examined in this study are under balancing selection in OWMs which prevents these markers from accurately resolving the evolutionary divergences between these species. However, previous research of gene regulation differences between species has found that while some drastic deviations in gene expression may be under directional or balancing selection (Whitehead and Crawford 2006; Romero et al. 2012), most inter-specific regulatory differences appear to be under stabilizing selection or neutral evolution (Brawand et al. 2011; Gilad 2012; Romero et al. 2012).

Inter-specific DMPs are found in genes enriched for functions associated with skeletal traits.

The evolution of methylation changes along specific NHP lineages is associated with several functions that may contribute to species-specific phenotypic differences (Files S6-S7). First, several skeletal tissue functions are enriched in species-specific DMPs. Among almost all NHPs, cellular adhesion functions are highly enriched. Cellular adhesion is necessary for cells to attach to other cells or extracellular matrix, which is a necessity for bone cells (Mbalaviele et al. 2006). Additionally, in baboons, chimpanzees, and marmosets, anatomical developmental processes are enriched, and in chimpanzees and marmosets, pattern specification processes, limb development, and skeletal system development are enriched. Lastly, in marmosets, specific skeletal functions, such as osteoblast differentiation and ossification are also enriched. Overall, these functions validate that most patterns of differential methylation relate to skeletal tissue function, regulation, development, and maintenance, as well to larger anatomical developmental processes. Additionally, functions not specific to the skeletal system were identified. In chimpanzees and marmosets, transcription and gene expression regulatory functions were enriched. Further, in marmosets, functions related to the development of skeletal muscles, nerves, the brain, the heart, blood vessels, kidneys, eyes, and ears were also enriched. All together, these findings suggest that many species-specific changes in methylation may contribute to the regulation of complex phenotypic changes. While this relationship was not observed for intra-specific skeletal morphology variation, other skeletal traits not examined in this study may be related. Nevertheless, many of the genes associated with the described

functions only contain an average of 1-2 differentially methylated sites. As described above, individual site-specific methylation changes are not readily associated with differential gene expression (Bork et al. 2010; Chen et al. 2011; Koch et al. 2011). Therefore, the enriched functions identified are likely not true biological effects due to methylation differences on their own. Rather they hint at biological effects that may be the result of the combined effects of several genetic, epigenetic, and other regulatory processes.

Finally, some of the genes containing species-specific DMPs overlap with those previously identified as being differentially methylated in other tissues among primates. Specifically, the neurotrophic factor *ARTN* shows species-specific hypomethylation at 1 site in marmosets, and in previous work it shows species-specific hypermethylation at 3 sites in humans as compared to other great apes (Hernando-Herraez et al. 2013). Additionally, *COL2A1* which codes for the predominant type of collagen in cartilage, shows species-specific hypermethylation at 3 sites in marmosets, and in previous work it shows species-specific hypermethylation of 4 sites in humans as compared to other great apes (Hernando-Herraez et al. 2013). The neuronal receptor *GABBR1* shows more complicated methylation patterns. In the current study, *GABBR1* shows species-specific hypermethylation at 2 sites in baboons, hypermethylation at 3 sites in marmosets, and hypomethylation at 2 sites in marmosets. In previous work, *GABBR1* shows hypomethylation in orangutans and hypermethylation in chimpanzees and bonobos (Hernando-Herraez et al. 2013). Lastly, 3 genes within the *HOXD* cluster, which are involved in limb development, also show complicated methylation patterns. In the current study, *HOXD8* shows species-specific hypermethylation at 3 sites in marmoset, *HOXD9* shows species-specific hypermethylation at 1 site in baboons and 2 sites in marmosets and species-specific hypomethylation at 2 sites in chimpanzees, and *HOXD10* shows species-specific hypermethylation at 5 sites in marmosets. In previous work, *HOXD8* shows hypomethylation in modern and archaic hominins while *HOXD9* and *HOXD10* show hypermethylation in archaic hominins as compared to modern humans (Gokhman et al. 2014).

In the *HOXD* cluster, *HOXD10* contains the largest number of NHP species-specific methylation differences observed in this study, has an active role in anatomical development, and has been found to be differentially methylated among hominins. Thus, it was selected for subsequent DNA methylation profiling and analysis at a higher resolution using gene-specific sequencing techniques. *HOXD10* specifically codes for a protein that functions as a sequence-specific transcription factor which is expressed in the developing limb buds and is involved in differentiation and limb development. In the current study, each NHP shows low to intermediate methylation levels across the gene body (Figure 5, Table S13). A similar pattern is observed in the gene-specific methylation data, which further reveals that *HOXD10* is not highly methylated in NHPs. However, across all taxa, some clusters of hypermethylation are found upstream of the gene and at the start of the gene body, with marmosets on average displaying more methylation in the gene body than other taxa (Figure 6, Table S18). In the *HOXD10* gene body of hominins, humans display hypomethylation, Neandertals displayed intermediate methylation levels, and Denisovans displayed high levels of methylation (Gokhman et al. 2014). The variation of methylation patterns in this gene body suggest that intermediate methylation levels may be a more ancestral epigenetic state for this region in the primate lineage, while the extreme hypermethylation of this region in Denisovans and the extreme hypomethylation of this region in humans may be derived epigenetic states. Previous work has proposed that methylation differences in *HOXD10* may be associated with phenotypic distinctions between modern human and archaic hominin limbs (Gokhman et al. 2014). While the current study did not find

substantial associations between methylation variation and aspects of femur morphology within NHP species, further work to understand the role of differential methylation of *HOXD10* in promoting morphological changes of the limb should be explored.

In conclusion, while only a few significant associations were identified between methylation and femur morphologies, several significant differences in methylation were observed inter-specifically. Moreover, these species-specific DMPs were found in genes enriched for functions associated with complex skeletal traits. This is the first study to characterize DNA methylation patterns in skeletal tissues from a taxonomically diverse set of NHPs, and it is the first study to directly compare these patterns to the nonpathological morphologies of the skeletal elements from which the tissues were derived. This design enabled an initial exploration of skeletal gene regulation and its relation to complex traits and species differences for which little else is currently known.

Materials and Methods:

Ethics Statement

NHP tissue samples included were opportunistically collected at routine necropsy of these animals. No animals were sacrificed for this study, and no living animals were used in this study. Chimpanzee tissues were collected opportunistically during routine necropsy prior to the September 2015 implementation of Fish and Wildlife Service rule 80 FR 34499.

NHP Samples

NHP samples come from captive colonies of chimpanzees (*Pan troglodytes*), baboons (*Papio spp.*), rhesus macaques (*Macaca mulatta*), and marmosets (*Callithrix jacchus*) from the Southwest National Primate Research Center in Texas, as well as vervets (*Chlorocebus aethiops*) from the Wake Forest/UCLA Vervet Research Colony in North Carolina. Femora were opportunistically collected at routine necropsy of these animals and stored in -20°C freezers at the Texas Biomedical Research Institute after dissection. These preparation and storage conditions ensured the preservation of skeletal DNA methylation patterns. Samples include baboons (n=28), macaques (n=10), vervets (n=10), chimpanzees (n=4), and marmosets (n=6). Age ranges span adulthood for each species and are comparable between each group (Figure 1, Table S1). Both sexes are represented (female: n=33, male: n=24, unknown: n=1).

Assessment of Femur Morphologies

On the right femora of NHP samples, 29 linear morphology traits (Figure 2, Table S6) were measured using calipers. These measurements characterize overall femur shape (McHenry and Corruccini 1978; Terzidis et al. 2012). Error for each measurement was determined by performing triplicate measurements on approximately 10% of the samples in each species. These measurements were spaced throughout the entire data collection period. Error was calculated as the mean absolute difference divided by the mean (Corner et al. 1992; White and Folkens 2000). All measurements that were retained for downstream analyses had errors of less than 5%, and the only measurement excluded was macaque intercondylar notch depth (error = 6.62%) (File S2).

Genome-Wide DNA Methylation Profiling

Trabecular bone cores were obtained from the medial condyles on the right distal femora of each NHP sample using a drill press that cored transversely through the condyle leaving the

526 articular surface preserved. Cortical bone was removed from cores using a Dremel, and the
527 remaining trabecular bone cores were pulverized into bone dust using a SPEX SamplePrep
528 Freezer/Mill. DNA was extracted from femoral trabecular bone using a phenol-chloroform
529 protocol optimized for skeletal tissues (Barnett and Larson 2012). Genome-wide DNA
530 methylation was assessed using Illumina Infinium MethylationEPIC microarrays (EPIC array)
531 (Supplemental Text). The array data discussed in this publication have been deposited in NCBI's
532 Gene Expression Omnibus and are accessible through GEO SuperSeries accession number
533 GSE103332, which includes the SubSeries accession numbers GSE103279, GSE103271,
534 GSE103280, GSE94677, GSE103328, and GSE103287.
535
536 ***Methylation Data Processing***
537 Using previously described methods (Housman et al. 2018), raw EPIC array data were
538 normalized and converted to β values which represent the average methylation levels at each site
539 (0 =completely unmethylated sites, 1 = fully methylated sites), and M values which are the log
540 transformed ratio of methylated signal to unmethylated signal. Probes with failed detection levels
541 (p-value > 0.05) in greater than 10% of samples and samples with greater than 30% of probes
542 with detection level failures were removed from downstream analyses. Using previously
543 described methods (Housman et al. 2018), probes with sequence mismatches to NHP genomes,
544 which could produce biased methylation measurements, were computationally filtered out and
545 excluded from downstream analyses (Supplemental Text, Figures S1-S3, Tables S2-S5, File S1).
546 Additionally, cross-reactive probes (McCartney et al. 2016), probes containing SNPs at the CpG
547 site, probes detecting SNP information, probes detecting methylation at non-CpG sites, and
548 probes targeting sites within the sex chromosomes were removed (Aryee et al. 2014; Fortin et al.
549 2016). This resulted in finalized datasets (Figure S4) that were used in further statistical analyses.
550
551 ***Statistical Analysis of Differential Methylation***
552 In order to identify sites that were significantly differentially methylated across
553 comparative groups, we designed and tested generalized linear mixed models (GLMMs) which
554 related the variables of interest (morphological measures and species membership) to the DNA
555 methylation patterns for each site, while accounting for the effects of additional variables, batch
556 effects, and latent variables (Maksimovic et al. 2016). Sites found to have significant
557 associations were classified as significant differentially methylated positions (DMPs).
558 Specifically, a GLMM was used to estimate differences in methylation levels associated with the
559 femur morphology within each taxonomic group (intra-specific) and between each taxonomic
560 group (inter-specific) (Supplemental Text).
561
562 ***Intra-Specific Analyses***
563 For the intra-specific analyses, variables included in each GLMM were the femur
564 morphologies within each taxonomic group, sex, age, and steady state weight when known, as
565 well as unknown latent variables calculated using the iteratively re-weighted least squares
566 approach in the sva package in R (Leek and Storey 2007; Leek and Storey 2008; Leek et al.
567 2012; Jaffe and Irizarry 2014). Latent variables estimated for each morphology were included to
568 help mitigate any unknown batch and cell heterogeneity effects on methylation variation at each
569 site (Table S7). Each GLMM design matrix was fit to corresponding M value array data by
570 generalized least squares using the limma package in R (Huber et al. 2015; Ritchie et al. 2015;
571 Phipson et al. 2016), and the estimated coefficients and standard errors for each morphology

were computed. Lastly, for each coefficient, an empirical Bayes approach (Lönnstedt and Speed 2002; Smyth 2004; McCarthy and Smyth 2009; Phipson et al. 2016) was used to compute moderated t-statistics, log-odds ratios of differential methylation, and associated p-values adjusted for multiple testing (Benjamini and Hochberg 1995). Significant DMPs for the effect of each morphology were defined as those having log fold changes in M values corresponding to an adjusted p-value of less than 0.05. Lastly, the gene ontology (GO) and KEGG pathway enrichment for significant CpGs was determined using the missMethyl package in R (Benjamini and Hochberg 1995; Young et al. 2010; Geeleher et al. 2013; Ritchie et al. 2015), which takes into account the differing number of probes per gene present on the array.

Inter-Specific Analyses

For the inter-specific analyses, variables included in the GLMM were taxonomic grouping, sex, age, known batch effects (e.g., array number and position), and unknown latent variables calculated using the method described above. The four latent variables estimated were included to help mitigate any unknown batch and cell heterogeneity effects on methylation variation at each site. The GLMM design matrix was fit to the M value array data using the method described above, and the estimated coefficients and standard errors for taxonomic group effects were computed. As described above, moderated t-statistics, log-odds ratios of differential methylation, and associated p-values adjusted for multiple testing were computed, and significant DMPs for the effect of taxonomy were defined as those having log fold changes in M values corresponding to an adjusted p-value of less than 0.05.

To determine only those methylation differences that represent fixed changes between genera, we used methods similar to those described in (Hernando-Herraez et al. 2013). Briefly, significant DMPs were identified between all possible pairwise comparisons of taxa (n=10: baboon-macaque, baboon-vervet, baboon-chimpanzee, baboon-marmoset, macaque-vervet, macaque-chimpanzee, macaque-marmoset, vervet-chimpanzee, vervet-marmoset, chimpanzee-marmoset). A significant DMP was then defined as taxon-specific if it was found to be significant in all four pairwise comparisons containing the taxon of interest but not found in any of the remaining pairwise comparisons. The GO and KEGG pathway enrichment of these DMPs was then determined as described above.

Additionally, global changes in methylation were calculated using distance matrices (Hernando-Herraez et al. 2013) of the methylation levels for all finalized 39,802 filtered probes. These changes were assessed at a species-level by averaging the β values per probe within each species. We then used Euclidean distances to calculate the difference between every two species. Neighbor joining trees were estimated from these distances using the ape package in R (Paradis et al. 2004). For each resulting tree, 1000 bootstraps were performed to determine confidence values for each branch. Global changes in methylation were also assessed at the individual-level using Euclidean distances to calculate the difference between every two individuals.

Gene-Specific DNA Methylation Profiling and Analyses

Based on the inter-specific DNA methylation patterns identified in this study and those identified in other evolutionary anthropological studies (Gokhman et al. 2014), the *HOXD10* gene was selected for subsequent DNA methylation profiling and analysis at a higher resolution using gene-specific sequencing techniques. Specifically, primers were designed and optimized to PCR amplify regions spanning across the entire *HOXD10* gene, as well as upstream and downstream several hundred bases (hg19 chr2:176980532-176985117), in each NHP species for

regular and bisulfite treated DNA (Tables S14-S17). All gene-specific assays were performed in a subset of the samples tested using the EPIC array and included chimpanzees (n=3), baboons (n=3), macaques (n=3), vervets (n=3), and marmosets (n=3) (Table S1). Additionally, a subset of these assays that targeted one validation locus (cg02193236) were performed in all of the samples (Table S1). As described above, DNA was extracted from femoral trabecular bone using a phenol-chloroform protocol optimized for skeletal tissues (Barnett and Larson 2012). DNA was bisulfite converted using the EZ DNA MethylationTM Gold Kit according to the manufacturer's instructions (Zymo Research). Successful PCR amplification was confirmed using gel electrophoresis. Gene-specific PCR products were then purified using an exonuclease I and shrimp alkaline phosphatase protocol and sequenced on the Applied Biosystems 3730 capillary sequencer at the DNA Laboratory at Arizona State University.

Regular and bisulfite sequences were aligned to the appropriate NHP references within the Enredo-Pecan-Orthus (EPO) whole-genome multiple alignments of several primate genomes [Ensembl Compara.8_primates_EPO] (Paten, Herrero, Beal, et al. 2008; Paten, Herrero, Fitzgerald, et al. 2008) using MEGA7 (Kumar et al. 2016). Manual annotation of these sequences within each sample confirmed that the gene sequences belong to the appropriate primate species and that the regular and bisulfite treated sequences only differ in cytosine composition. The number and distribution of methylated loci throughout the *HOXD10* gene were then identified compared within and among species to provide a higher resolution of methylation variation within this targeted gene. Lastly, with respect to the validation locus (cg02193236) evaluated in all samples, methylation levels across this region were confirmed to correspond with the methylation levels of this region as determined using the EPIC array.

Acknowledgements and Funding Information:

This work was supported by the National Institutes of Health (P01 HL028972 to Anthony G. Comuzzie); the Leakey Foundation (Research Grant for Doctoral Students to G.H.); the Wenner-Gren Foundation (Gr. 9310 to G.H.); the Nacey Maggioncalda Foundation (James F. Nacey Fellowship to G.H.); the International Primatological Society (to G.H.); Sigma Xi (Grant-in-Aid of Research to G.H.); the ASU Center for Evolution and Medicine (Venture Fund to G.H.); the ASU Graduate Research and Support Program (to G.H.). Additionally, this investigation used resources that were supported by the Southwest National Primate Research Center grant P51 OD011133 from the Office of Research Infrastructure Programs, National Institutes of Health.

We thank Eric D. Johnson and members of the Department of Genetics at the Texas Biomedical Research Institute, including Anthony G. Comuzzie, Anne Sheldrake, Jaydee Foster, Kara Peterson, Mel Carless, and Laura Cox, for helpful discussions. We also thank Megann Phillips for assistance with PCR primer design.

Newly reported data have been made available on NCBI's Gene Expression Omnibus and are accessible through the GEO SuperSeries accession number GSE103332, which includes the following SubSeries accession numbers: GSE103279 (intra-specific baboon DNA methylation data), GSE103271 (intra-specific macaque DNA methylation data), GSE103280 (intra-specific vervet DNA methylation data), GSE94677 (intra-specific chimp DNA methylation data), GSE103328 (intra-specific marmoset DNA methylation data), and GSE103287 (inter-specific DNA methylation data).

References:

de Andrés MC, Kingham E, Imagawa K, Gonzalez A, Roach HI, Wilson DI, Oreffo ROC. 2013. Epigenetic Regulation during Fetal Femur Development: DNA Methylation Matters.Neves NM, editor. PLoS ONE 8:e54957.

Ankel-Simons F. 2007. Primate Anatomy. 3rd ed. New York: Academic Press

Aryee MJ, Jaffe AE, Corrada-Bravo H, Ladd-Acosta C, Feinberg AP, Hansen KD, Irizarry RA. 2014. Minfi: a flexible and comprehensive Bioconductor package for the analysis of Infinium DNA methylation microarrays. Bioinformatics 30:1363–1369.

Babbitt CC, Fedrigo O, Pfefferle AD, Boyle AP, Horvath JE, Furey TS, Wray GA. 2010. Both Noncoding and Protein-Coding RNAs Contribute to Gene Expression Evolution in the Primate Brain. Genome Biol. Evol. 2:67–79.

Bell CG, Wilson GA, Butcher LM, Roos C, Walter L, Beck S. 2012. Human-specific CpG "beacons" identify loci associated with human-specific traits and disease. Epigenetics 7:1188–1199.

Benjamini Y, Hochberg Y. 1995. Controlling the False Discovery Rate: A Practical and Powerful Approach to Multiple Testing. J. R. Stat. Soc. Ser. B Methodol. 57:289–300.

Blekhman R, Oshlack A, Chabot AE, Smyth GK, Gilad Y. 2008. Gene Regulation in Primates Evolves under Tissue-Specific Selection Pressures.McVean G, editor. PLoS Genet. 4:e1000271.

Bork S, Pfister S, Witt H, Horn P, Korn B, Ho AD, Wagner W. 2010. DNA methylation pattern changes upon long-term culture and aging of human mesenchymal stromal cells. Aging Cell 9:54–63.

Bovée JVMG, Hogendoorn PCW, Wunder JS, Alman BA. 2010. Cartilage tumours and bone development: molecular pathology and possible therapeutic targets. Nat. Rev. Cancer 10:481–488.

Brand-Saberi B. 2005. Genetic and epigenetic control of skeletal muscle development. Ann. Anat. - Anat. Anz. 187:199–207.

Brawand D, Soumillon M, Necsulea A, Julien P, Csárdi G, Harrigan P, Weier M, Liechti A, Aximu-Petri A, Kircher M, et al. 2011. The evolution of gene expression levels in mammalian organs. Nature 478:343–348.

Cáceres M, Lachuer J, Zapala MA, Redmond JC, Kudo L, Geschwind DH, Lockhart DJ, Preuss TM, Barlow C. 2003. Elevated gene expression levels distinguish human from non-human primate brains. Proc. Natl. Acad. Sci. 100:13030–13035.

Cawthon Lang KA. 2005. Primate Factsheets: Common marmoset (Callithrix jacchus) Taxonomy, Morphology, & Ecology. Available from: http://pin.primate.wisc.edu/factsheets/entry/common_marmoset

Cawthon Lang KA. 2006. Primate Factsheets: Chimpanzee (Pan troglodytes) Taxonomy, Morphology, & Ecology. Available from: http://pin.primate.wisc.edu/factsheets/entry/chimpanzee

Chen Y, Choufani S, Ferreira JC, Grafodatskaya D, Butcher DT, Weksberg R. 2011. Sequence overlap between autosomal and sex-linked probes on the Illumina HumanMethylation27 microarray. Genomics 97:214–222.

Corner B, Lele S, Richtsmeier J. 1992. Measuring precision of three-dimensional landmark data. J. Quant. Anthropol. 3:347–359.

Delgado-Calle J, Fernández AF, Sainz J, Zarrabeitia MT, Sañudo C, García-Renedo R, Pérez-Núñez MI, García-Ibarbia C, Fraga MF, Riancho JA. 2013. Genome-wide profiling of

bone reveals differentially methylated regions in osteoporosis and osteoarthritis. Arthritis Rheum. 65:197–205.

Dimitriou R, Jones E, McGonagle D, Giannoudis PV. 2011. Bone regeneration: current concepts and future directions. BMC Med. 9:1.

van Dongen J, Ehli E, Slieker R, Bartels M, Weber Z, Davies G, Slagboom P, Heijmans B, Boomsma D. 2014. Epigenetic Variation in Monozygotic Twins: A Genome-Wide Analysis of DNA Methylation in Buccal Cells. Genes 5:347–365.

Elango N, Lee J, Peng Z, Loh Y-HE, Yi SV. 2009. Evolutionary rate variation in Old World monkeys. Biol. Lett. 5:405–408.

Elango N, Thomas JW, Program‡§ NCS, Yi SV. 2006. Variable molecular clocks in hominoids. Proc. Natl. Acad. Sci. 103:1370–1375.

Enard W, Fassbender A, Model F, Adorján P, Pääbo S, Olek A. 2004. Differences in DNA methylation patterns between humans and chimpanzees. Curr. Biol. 14:R148–R149.

Farcas R, Schneider E, Frauenknecht K, Kondova I, Bontrop R, Bohl J, Navarro B, Metzler M, Zischler H, Zechner U, et al. 2009. Differences in DNA Methylation Patterns and Expression of the CCRK Gene in Human and Nonhuman Primate Cortices. Mol. Biol. Evol. 26:1379–1389.

Fernández-Tajes J, Soto-Hermida A, Vázquez-Mosquera ME, Cortés-Pereira E, Mosquera A, Fernández-Moreno M, Oreiro N, Fernández-López C, Fernández JL, Rego-Pérez I, et al. 2014. Genome-wide DNA methylation analysis of articular chondrocytes reveals a cluster of osteoarthritic patients. Ann. Rheum. Dis. 73:668–677.

Flanagan JM, Popendikyte V, Pozdniakovaite N, Sobolev M, Assadzadeh A, Schumacher A, Zangeneh M, Lau L, Virtanen C, Wang S-C, et al. 2006. Intra- and Interindividual Epigenetic Variation in Human Germ Cells. Am. J. Hum. Genet. 79:67–84.

Fleagle JG. 1999. Primate Adaptation and Evolution. New York: Academic Press

Fortin J-P, Triche T, Hansen K. 2016. Preprocessing, normalization and integration of the Illumina HumanMethylationEPIC array. bioRxiv:065490.

Fraga MF, Ballestar E, Paz MF, Ropero S, Setien F, Ballestar ML, Heine-Suñer D, Cigudosa JC, Urioste M, Benitez J, et al. 2005. Epigenetic differences arise during the lifetime of monozygotic twins. Proc. Natl. Acad. Sci. U. S. A. 102:10604–10609.

Fukuda K, Ichiyanagi K, Yamada Y, Go Y, Udono T, Wada S, Maeda T, Soejima H, Saitou N, Ito T, et al. 2013. Regional DNA methylation differences between humans and chimpanzees are associated with genetic changes, transcriptional divergence and disease genes. J. Hum. Genet. 58:446–454.

Gama-Sosa MA, Midgett RM, Slagel VA, Githens S, Kuo KC, Gehrke CW, Ehrlich M. 1983. Tissue-specific differences in DNA methylation in various mammals. Biochim. Biophys. Acta BBA-Gene Struct. Expr. 740:212–219.

Gao F, Niu Y, Sun YE, Lu H, Chen Y, Li S, Kang Y, Luo Y, Si C, Yu J, et al. 2017. De novo DNA methylation during monkey pre-implantation embryogenesis. Cell Res. [Internet]. Available from: http://www.nature.com/cr/journal/vaop/ncurrent/full/cr201725a.html

García-Ibarbia C, Delgado-Calle J, Casafont I, Velasco J, Arozamena J, Pérez-Núñez MI, Alonso MA, Berciano MT, Ortiz F, Pérez-Castrillón JL, et al. 2013. Contribution of genetic and epigenetic mechanisms to Wnt pathway activity in prevalent skeletal disorders. Gene 532:165–172.

753 Geeleher P, Hartnett L, Egan LJ, Golden A, Raja Ali RA, Seoighe C. 2013. Gene-set analysis is
754 severely biased when applied to genome-wide methylation data. Bioinforma. Oxf. Engl.
755 29:1851–1857.
756 Gibbs JR, van der Brug MP, Hernandez DG, Traynor BJ, Nalls MA, Lai S-L, Arepalli S,
757 Dillman A, Rafferty IP, Troncoso J, et al. 2010. Abundant Quantitative Trait Loci Exist
758 for DNA Methylation and Gene Expression in Human Brain.Flint J, editor. PLoS Genet.
759 6:e1000952.
760 Gilad Y. 2012. Using Genomic Tools to Study Regulatory Evolution. Methods Mol. Biol. Clifton
761 NJ 856:335–361.
762 Gokhman D, Agranat-Tamir L, Housman G, Garcia-Perez R, Nissim-Rafinia M, Mallick S,
763 Nieves-Colón M, Li H, Alpaslan-Roodenberg S, Novak M, et al. 2017. Extensive
764 Regulatory Changes in Genes Affecting Vocal and Facial Anatomy Separate Modern
765 from Archaic Humans. bioRxiv:106955.
766 Gokhman D, Lavi E, Prüfer K, Fraga MF, Riancho JA, Kelso J, Pääbo S, Meshorer E, Carmel L.
767 2014. Reconstructing the DNA methylation maps of the Neandertal and the Denisovan.
768 Science 344:523–527.
769 Gokhman D, Meshorer E, Carmel L. 2016. Epigenetics: It's Getting Old. Past Meets Future in
770 Paleoepigenetics. Trends Ecol. Evol. 31:290–300.
771 Goldring MB, Marcu KB. 2012. Epigenomic and microRNA-mediated regulation in cartilage
772 development, homeostasis, and osteoarthritis. Trends Mol. Med. 18:109–118.
773 Haygood R, Fedrigo O, Hanson B, Yokoyama K-D, Wray GA. 2007. Promoter regions of many
774 neural- and nutrition-related genes have experienced positive selection during human
775 evolution. Nat. Genet. 39:1140–1144.
776 Henriksen M, Creaby MW, Lund H, Juhl C, Christensen R. 2014. Is there a causal link between
777 knee loading and knee osteoarthritis progression? A systematic review and meta-analysis
778 of cohort studies and randomised trials. BMJ Open 4:e005368.
779 Hernando-Herraez I, Prado-Martinez J, Garg P, Fernandez-Callejo M, Heyn H, Hvilsom C,
780 Navarro A, Esteller M, Sharp AJ, Marques-Bonet T. 2013. Dynamics of DNA
781 Methylation in Recent Human and Great Ape Evolution. PLOS Genet 9:e1003763.
782 Heyn H, Moran S, Hernando-Herraez I, Sayols S, Gomez A, Sandoval J, Monk D, Hata K,
783 Marques-Bonet T, Wang L, et al. 2013. DNA methylation contributes to natural human
784 variation. Genome Res. 23:1363–1372.
785 den Hollander W, Ramos YFM, Bos SD, Bomer N, van der Breggen R, Lakenberg N, de Dijcker
786 WJ, Duijnisveld BJ, Slagboom PE, Nelissen RGHH, et al. 2014. Knee and hip articular
787 cartilage have distinct epigenomic landscapes: implications for future cartilage
788 regeneration approaches. Ann. Rheum. Dis. 73:2208–2212.
789 Housman G, Havill LM, Quillen EE, Comuzzie AG, Stone AC. 2018. Assessment of DNA
790 Methylation Patterns in the Bone and Cartilage of a Nonhuman Primate Model of
791 Osteoarthritis. CARTILAGE [Internet]. Available from:
792 http://journals.sagepub.com/eprint/UzBEFuVaATyPnanB3shB/full
793 Huber W, Carey VJ, Gentleman R, Anders S, Carlson M, Carvalho BS, Bravo HC, Davis S,
794 Gatto L, Girke T, et al. 2015. Orchestrating high-throughput genomic analysis with
795 Bioconductor. Nat. Methods 12:115–121.
796 Iliopoulos D, Malizos KN, Oikonomou P, Tsezou A. 2008. Integrative MicroRNA and
797 Proteomic Approaches Identify Novel Osteoarthritis Genes and Their Collaborative
798 Metabolic and Inflammatory Networks.Koutsopoulos S, editor. PLoS ONE 3:e3740.

Jacob RA, Gretz DM, Taylor PC, James SJ, Pogribny IP, Miller BJ, Henning SM, Swendseid ME. 1998. Moderate folate depletion increases plasma homocysteine and decreases lymphocyte DNA methylation in postmenopausal women. J. Nutr. 128:1204–1212.

Jaffe AE, Irizarry RA. 2014. Accounting for cellular heterogeneity is critical in epigenome-wide association studies. Genome Biol. 15:R31.

Jeffries MA, Donica M, Baker LW, Stevenson ME, Annan AC, Beth Humphrey M, James JA, Sawalha AH. 2016. Genome-Wide DNA Methylation Study Identifies Significant Epigenomic Changes in Osteoarthritic Subchondral Bone and Similarity to Overlying Cartilage. Arthritis Rheumatol. 68:1403–1414.

Jeffries MA, Donica M, Baker LW, Stevenson ME, Annan AC, Humphrey MB, James JA, Sawalha AH. 2014. Genome-Wide DNA Methylation Study Identifies Significant Epigenomic Changes in Osteoarthritic Cartilage. Arthritis Rheumatol. 66:2804–2815.

Joganic JL, Willmore KE, Richtsmeier JT, Weiss KM, Mahaney MC, Rogers J, Cheverud JM. 2017. Additive genetic variation in the craniofacial skeleton of baboons (genus Papio) and its relationship to body and cranial size. Am. J. Phys. Anthropol.:1–17.

Karere GM, Glenn JP, Birnbaum S, Rainwater DL, Mahaney MC, VandeBerg JL, Cox LA. 2013. Identification of candidate genes encoding an LDL-C QTL in baboons. J. Lipid Res. 54:1776–1785.

Karere GM, Glenn JP, VandeBerg JL, Cox LA. 2010. Identification of baboon microRNAs expressed in liver and lymphocytes. J. Biomed. Sci. 17:1.

Karere GM, Glenn JP, VandeBerg JL, Cox LA. 2012. Differential microRNA response to a high-cholesterol, high-fat diet in livers of low and high LDL-C baboons. BMC Genomics 13:1.

Kasaai B, Gaumond M-H, Moffatt P. 2013. Regulation of the Bone-restricted IFITM-like (Bril) Gene Transcription by Sp and Gli Family Members and CpG Methylation. J. Biol. Chem. 288:13278–13294.

King MC, Wilson AC. 1975. Evolution at two levels in humans and chimpanzees. Science 188:107–116.

Koch CM, Suschek CV, Lin Q, Bork S, Goergens M, Joussen S, Pallua N, Ho AD, Zenke M, Wagner W. 2011. Specific Age-Associated DNA Methylation Changes in Human Dermal Fibroblasts. PLOS ONE 6:e16679.

Kothapalli KSD, Anthony JC, Pan BS, Hsieh AT, Nathanielsz PW, Brenna JT. 2007. Differential Cerebral Cortex Transcriptomes of Baboon Neonates Consuming Moderate and High Docosahexaenoic Acid Formulas.Akbarian S, editor. PLoS ONE 2:e370.

Lea AJ, Altmann J, Alberts SC, Tung J. 2016. Resource base influences genome-wide DNA methylation levels in wild baboons (Papio cynocephalus). Mol. Ecol. 25:1681–1696.

Leek JT, Johnson WE, Parker HS, Jaffe AE, Storey JD. 2012. The sva package for removing batch effects and other unwanted variation in high-throughput experiments. Bioinformatics 28:882–883.

Leek JT, Storey JD. 2007. Capturing Heterogeneity in Gene Expression Studies by Surrogate Variable Analysis. PLoS Genet. 3:e161.

Leek JT, Storey JD. 2008. A general framework for multiple testing dependence. Proc. Natl. Acad. Sci. 105:18718–18723.

Leigh SR, Shea BT. 1995. Ontogeny and the evolution of adult body size dimorphism in apes. Am. J. Primatol. 36:37–60.

Lewton KL. 2017. The effects of captive versus wild rearing environments on long bone articular surfaces in common chimpanzees (Pan troglodytes). PeerJ 5:e3668.

Lewton KL, Ritzman T, Copes LE, Garland T, Capellini TD. 2018. Exercise-induced loading increases ilium cortical area in a selectively bred mouse model. Am. J. Phys. Anthropol.:1–9.

Lindskog C, Kuhlwilm M, Davierwala A, Fu N, Hegde G, Uhlén M, Navani S, Pääbo S, Pontén F. 2014. Analysis of candidate genes for lineage-specific expression changes in humans and primates. J. Proteome Res. 13:3596–3606.

Ling BMT, Bharathy N, Chung T-K, Kok WK, Li S, Tan YH, Rao VK, Gopinadhan S, Sartorelli V, Walsh MJ, et al. 2012. Lysine methyltransferase G9a methylates the transcription factor MyoD and regulates skeletal muscle differentiation. Proc. Natl. Acad. Sci. 109:841–846.

Lister R, Pelizzola M, Dowen RH, Hawkins RD, Hon G, Tonti-Filippini J, Nery JR, Lee L, Ye Z, Ngo Q-M, et al. 2009. Human DNA methylomes at base resolution show widespread epigenomic differences. Nature 462:315–322.

Liu Y, Aryee MJ, Padyukov L, Fallin MD, Hesselberg E, Runarsson A, Reinius L, Acevedo N, Taub M, Ronninger M, et al. 2013. Epigenome-wide association data implicate DNA methylation as an intermediary of genetic risk in rheumatoid arthritis. Nat. Biotechnol. 31:142–147.

Lönnstedt I, Speed T. 2002. Replicated microarray data. Stat. Sin. 12:31–46.

Loughlin J, Reynard LN. 2015. Osteoarthritis: Epigenetics of articular cartilage in knee and hip OA. Nat. Rev. Rheumatol. 11:6–7.

Macrini TE, Coan HB, Levine SM, Lerma T, Saks CD, Araujo DJ, Bredbenner TL, Coutts RD, Nicolella DP, Havill LM. 2013. Reproductive status and sex show strong effects on knee OA in a baboon model. Osteoarthr. Cartil. OARS Osteoarthr. Res. Soc. 21:839–848.

Madrid A, Chopra P, Alisch RS. 2018. Species-Specific 5 mC and 5 hmC Genomic Landscapes Indicate Epigenetic Contribution to Human Brain Evolution. Front. Mol. Neurosci. [Internet] 11. Available from: https://www.frontiersin.org/articles/10.3389/fnmol.2018.00039/full

Maksimovic J, Phipson B, Oshlack A. 2016. A cross-package Bioconductor workflow for analysing methylation array data. F1000Research 5:1281.

Martin DIK, Singer M, Dhahbi J, Mao G, Zhang L, Schroth GP, Pachter L, Boffelli D. 2011. Phyloepigenomic comparison of great apes reveals a correlation between somatic and germline methylation states. Genome Res. 21:2049–2057.

Mbalaviele G, Shin CS, Civitelli R. 2006. Perspective: Cell–Cell Adhesion and Signaling Through Cadherins: Connecting Bone Cells in Their Microenvironment. J. Bone Miner. Res. 21:1821–1827.

McCarthy DJ, Smyth GK. 2009. Testing significance relative to a fold-change threshold is a TREAT. Bioinformatics 25:765–771.

McCartney DL, Walker RM, Morris SW, McIntosh AM, Porteous DJ, Evans KL. 2016. Identification of polymorphic and off-target probe binding sites on the Illumina Infinium MethylationEPIC BeadChip. Genomics Data 9:22–24.

McHenry HM, Corruccini RS. 1978. The femur in early human evolution. Am. J. Phys. Anthropol. 49:473–487.

Mendizabal I, Shi L, Keller TE, Konopka G, Preuss TM, Hsieh T-F, Hu E, Zhang Z, Su B, Yi SV. 2016. Comparative Methylome Analyses Identify Epigenetic Regulatory Loci of Human Brain Evolution. Mol. Biol. Evol. 33:2947–2959.

Moazedi-Fuerst FC, Hofner M, Gruber G, Weinhaeusel A, Stradner MH, Angerer H, Peischler D, Lohberger B, Glehr M, Leithner A, et al. 2014. Epigenetic differences in human cartilage between mild and severe OA. J. Orthop. Res. 32:1636–1645.

Molaro A, Hodges E, Fang F, Song Q, McCombie WR, Hannon GJ, Smith AD. 2011. Sperm Methylation Profiles Reveal Features of Epigenetic Inheritance and Evolution in Primates. Cell 146:1029–1041.

Morris JA, Tsai P-C, Joehanes R, Zheng J, Trajanoska K, Soerensen M, Forgetta V, Castillo-Fernandez JE, Frost M, Spector TD, et al. 2017. Epigenome-wide association of DNA methylation in whole blood with bone mineral density. J. Bone Miner. Res.:n/a-n/a.

Oates NA, van Vliet J, Duffy DL, Kroes HY, Martin NG, Boomsma DI, Campbell M, Coulthard MG, Whitelaw E, Chong S. 2006. Increased DNA Methylation at the AXIN1 Gene in a Monozygotic Twin from a Pair Discordant for a Caudal Duplication Anomaly. Am. J. Hum. Genet. 79:155–162.

Ostanek B, Kranjc T, Lovšin N, Zupan J, Marc J. 2018. Chapter 18 - Epigenetic Mechanisms in Osteoporosis. In: Moskalev A, Vaiserman AM, editors. Epigenetics of Aging and Longevity. Translational Epigenetics. Boston: Academic Press. p. 365–388. Available from: https://www.sciencedirect.com/science/article/pii/B9780128110607000188

Pai AA, Bell JT, Marioni JC, Pritchard JK, Gilad Y. 2011. A Genome-Wide Study of DNA Methylation Patterns and Gene Expression Levels in Multiple Human and Chimpanzee Tissues. PLOS Genet. 7:e1001316.

Palacios D, Puri PL. 2006. The epigenetic network regulating muscle development and regeneration. J. Cell. Physiol. 207:1–11.

Pandorf CE, Haddad F, Wright C, Bodell PW, Baldwin KM. 2009. Differential epigenetic modifications of histones at the myosin heavy chain genes in fast and slow skeletal muscle fibers and in response to muscle unloading. AJP Cell Physiol. 297:C6–C16.

Paradis E, Claude J, Strimmer K. 2004. APE: Analyses of Phylogenetics and Evolution in R language. Bioinforma. Oxf. Engl. 20:289–290.

Perelman P, Johnson WE, Roos C, Seuánez HN, Horvath JE, Moreira MAM, Kessing B, Pontius J, Roelke M, Rumpler Y, et al. 2011. A Molecular Phylogeny of Living Primates.Brosius J, editor. PLoS Genet. 7:e1001342.

Petronis A, Gottesman II, Kan P, Kennedy JL, Basile VS, Paterson AD, Popendikyte V. 2003. Monozygotic twins exhibit numerous epigenetic differences: clues to twin discordance? Schizophr. Bull. 29:169–178.

Phipson B, Lee S, Majewski IJ, Alexander WS, Smyth GK. 2016. Robust hyperparameter estimation protects against hypervariable genes and improves power to detect differential expression. Ann. Appl. Stat. 10:946–963.

Prendergast JG, Campbell H, Gilbert N, Dunlop MG, Bickmore WA, Semple CA. 2007. Chromatin structure and evolution in the human genome. BMC Evol. Biol. 7:72.

Provencal N, Suderman MJ, Guillemin C, Massart R, Ruggiero A, Wang D, Bennett AJ, Pierre PJ, Friedman DP, Cote SM, et al. 2012. The Signature of Maternal Rearing in the Methylome in Rhesus Macaque Prefrontal Cortex and T Cells. J. Neurosci. 32:15626–15642.

Rakyan VK, Hildmann T, Novik KL, Lewin J, Tost J, Cox AV, Andrews TD, Howe KL, Otto T, Olek A, et al. 2004. DNA Methylation Profiling of the Human Major Histocompatibility Complex: A Pilot Study for the Human Epigenome Project. PLOS Biol. 2:e405.

Ralston SH, Uitterlinden AG. 2010. Genetics of Osteoporosis. Endocr. Rev. 31:629–662.

936 Ramos YFM, den Hollander W, Bovée JVMG, Bomer N, van der Breggen R, Lakenberg N,
937 Keurentjes JC, Goeman JJ, Slagboom PE, Nelissen RGHH, et al. 2014. Genes Involved
938 in the Osteoarthritis Process Identified through Genome Wide Expression Analysis in
939 Articular Cartilage; the RAAK Study. PLoS ONE 9:1–12.
940 Rampersaud GC, Kauwell GP, Hutson AD, Cerda JJ, Bailey LB. 2000. Genomic DNA
941 methylation decreases in response to moderate folate depletion in elderly women. Am. J.
942 Clin. Nutr. 72:998–1003.
943 Reynard LN. 2017. Analysis of genetics and DNA methylation in osteoarthritis: What have we
944 learnt about the disease? Semin. Cell Dev. Biol. 62:57–66.
945 Reynard LN, Bui C, Syddall CM, Loughlin J. 2014. CpG methylation regulates allelic expression
946 of GDF5 by modulating binding of SP1 and SP3 repressor proteins to the osteoarthritis
947 susceptibility SNP rs143383. Hum. Genet. 133:1059–1073.
948 Ritchie ME, Phipson B, Wu D, Hu Y, Law CW, Shi W, Smyth GK. 2015. limma powers
949 differential expression analyses for RNA-sequencing and microarray studies. Nucleic
950 Acids Res.:gkv007.
951 Ritzman TB, Banovich N, Buss KP, Guida J, Rubel MA, Pinney J, Khang B, Ravosa MJ, Stone
952 AC. 2017. Facing the facts: The Runx2 gene is associated with variation in facial
953 morphology in primates. J. Hum. Evol. 111:139–151.
954 Rivadeneira F, Styrkársdottir U, Estrada K, Halldórsson BV, Hsu Y-H, Richards JB, Zillikens
955 MC, Kavvoura FK, Amin N, Aulchenko YS, et al. 2009. Twenty bone-mineral-density
956 loci identified by large-scale meta-analysis of genome-wide association studies. Nat.
957 Genet. 41:1199–1206.
958 Rogers J, Gibbs RA. 2014. Comparative primate genomics: emerging patterns of genome content
959 and dynamics. Nat. Rev. Genet. 15:347–359.
960 Romero IG, Ruvinsky I, Gilad Y. 2012. Comparative studies of gene expression and the
961 evolution of gene regulation. Nat. Rev. Genet. 13:505–516.
962 Rushton MD, Reynard LN, Barter MJ, Refaie R, Rankin KS, Young DA, Loughlin J. 2014.
963 Characterization of the Cartilage DNA Methylome in Knee and Hip Osteoarthritis:
964 Methylation Profile of OA Cartilage. Arthritis Rheumatol. 66:2450–2460.
965 Schultz AH. 1930. The Skeleton of the Trunk and Limbs of Higher Primates. Hum. Biol. 2:303–
966 438.
967 Schultz AH. 1937. Proportions, Variability and Asymmetries of the Long Bones of the Limbs
968 and the Clavicles in Man and Apes. Hum. Biol. 9:281–328.
969 Sharif J, Endo TA, Toyoda T, Koseki H. 2010. Divergence of CpG island promoters: A
970 consequence or cause of evolution? Dev. Growth Differ. 52:545–554.
971 Shelnutt KP, Kauwell GPA, Gregory III JF, Maneval DR, Quinlivan EP, Theriaque DW,
972 Henderson GN, Bailey LB. 2004. Methylenetetrahydrofolate reductase 677C→T
973 polymorphism affects DNA methylation in response to controlled folate intake in young
974 women. J. Nutr. Biochem. 15:554–560.
975 Simon TC, Jeffries MA. 2017. The Epigenomic Landscape in Osteoarthritis. Curr. Rheumatol.
976 Rep. 19:30.
977 Singer M, Kosti I, Pachter L, Mandel-Gutfreund Y. 2015. A diverse epigenetic landscape at
978 human exons with implication for expression. Nucleic Acids Res.:gkv153.
979 Slieker RC, Bos SD, Goeman JJ, Bovée JV, Talens RP, van der Breggen R, Suchiman HED,
980 Lameijer E-W, Putter H, van den Akker EB, et al. 2013. Identification and systematic

annotation of tissue-specific differentially methylated regions using the Illumina 450k array. Epigenetics Chromatin 6:26.

Smith RWA, Monroe C, Bolnick DA. 2015. Detection of Cytosine Methylation in Ancient DNA from Five Native American Populations Using Bisulfite Sequencing. PLoS ONE [Internet] 10. Available from: http://www.ncbi.nlm.nih.gov/pmc/articles/PMC4445908/

Smith SM, Garic A, Berres ME, Flentke GR. 2014. Genomic factors that shape craniofacial outcome and neural crest vulnerability in FASD. Front. Genet. [Internet] 5. Available from: http://journal.frontiersin.org/article/10.3389/fgene.2014.00224/abstract

Smyth GK. 2004. Linear models and empirical bayes methods for assessing differential expression in microarray experiments. Stat. Appl. Genet. Mol. Biol. 3:Article3.

Suter CM, Martin DIK, Ward RL. 2004. Germline epimutation of MLH1 in individuals with multiple cancers. Nat. Genet. 36:497–501.

Suzuki MM, Bird A. 2008. DNA methylation landscapes: provocative insights from epigenomics. Nat. Rev. Genet. 9:465–476.

Terzidis I, Totlis T, Papathanasiou E, Sideridis A, Vlasis K, Natsis K. 2012. Gender and Side-to-Side Differences of Femoral Condyles Morphology: Osteometric Data from 360 Caucasian Dried Femori. Anat. Res. Int. 2012:e679658.

Tung J, Zhou X, Alberts SC, Stephens M, Gilad Y. 2015. The genetic architecture of gene expression levels in wild baboons. eLife 4:e04729.

Uebbing S, Künstner A, Mäkinen H, Backström N, Bolivar P, Burri R, Dutoit L, Mugal CF, Nater A, Aken B, et al. 2016. Divergence in gene expression within and between two closely related flycatcher species. Mol. Ecol. 25:2015–2028.

Vilgalys TP, Rogers J, Jolly C, Mukherjee S, Tung J. 2018. Evolution of DNA methylation in baboons. Available from: http://biorxiv.org/lookup/doi/10.1101/400093

Warner LR, Babbitt CC, Primus AE, Severson TF, Haygood R, Wray GA. 2009. Functional consequences of genetic variation in primates on tyrosine hydroxylase (TH) expression in vitro. Brain Res. 1288:1–8.

Weber M, Hellmann I, Stadler MB, Ramos L, Pääbo S, Rebhan M, Schübeler D. 2007. Distribution, silencing potential and evolutionary impact of promoter DNA methylation in the human genome. Nat. Genet. 39:457–466.

Weksberg R, Shuman C, Caluseriu O, Smith AC, Fei Y-L, Nishikawa J, Stockley TL, Best L, Chitayat D, Olney A, et al. 2002. Discordant KCNQ1OT1 imprinting in sets of monozygotic twins discordant for Beckwith-Wiedemann syndrome. Hum. Mol. Genet. 11:1317–1325.

White T, Folkens P. 2000. Human osteology. 2nd ed. San Diego: Academic Press

Whitehead A, Crawford DL. 2006. Neutral and adaptive variation in gene expression. Proc. Natl. Acad. Sci. U. S. A. 103:5425–5430.

Young MD, Wakefield MJ, Smyth GK, Oshlack A. 2010. Gene ontology analysis for RNA-seq: accounting for selection bias. Genome Biol. 11:R14.

Zeng J, Konopka G, Hunt BG, Preuss TM, Geschwind D, Yi SV. 2012. Divergent Whole-Genome Methylation Maps of Human and Chimpanzee Brains Reveal Epigenetic Basis of Human Regulatory Evolution. Am. J. Hum. Genet. 91:455–465.

Zhang Bo, Zhou Y, Lin N, Lowdon RF, Hong C, Nagarajan RP, Cheng JB, Li D, Stevens M, Lee HJ, et al. 2013. Functional DNA methylation differences between tissues, cell types, and across individuals discovered using the M&M algorithm. Genome Res. 23:1522–1540.

Zwetsloot KA, Laye MJ, Booth FW. 2009. Novel epigenetic regulation of skeletal muscle myosin heavy chain genes. Focus on "Differential epigenetic modifications of histones at the myosin heavy chain genes in fast and slow skeletal muscle fibers and in response to muscle unloading." AJP Cell Physiol. 297:C1–C3.

Figures:

Figure 1.

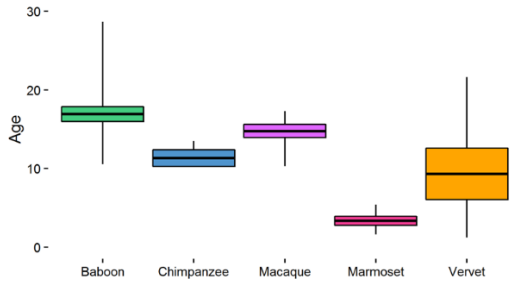

Figure 2.

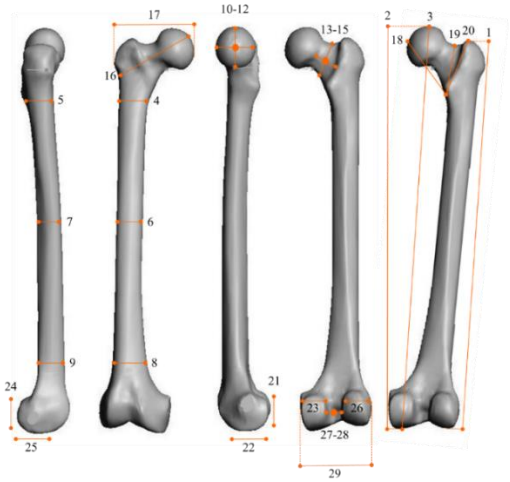

Figure 3.

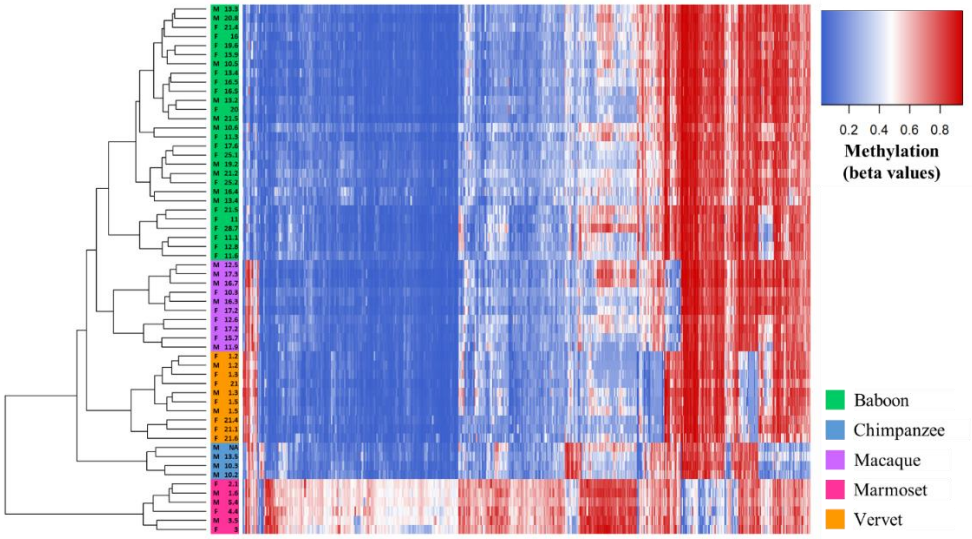

Figure 4.

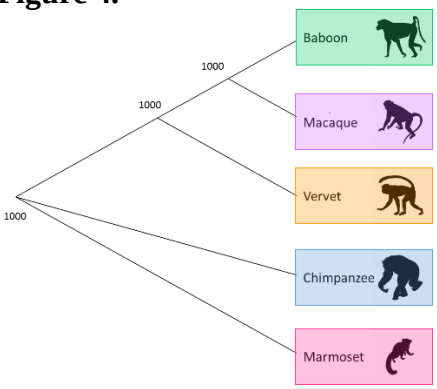

Figure 5.

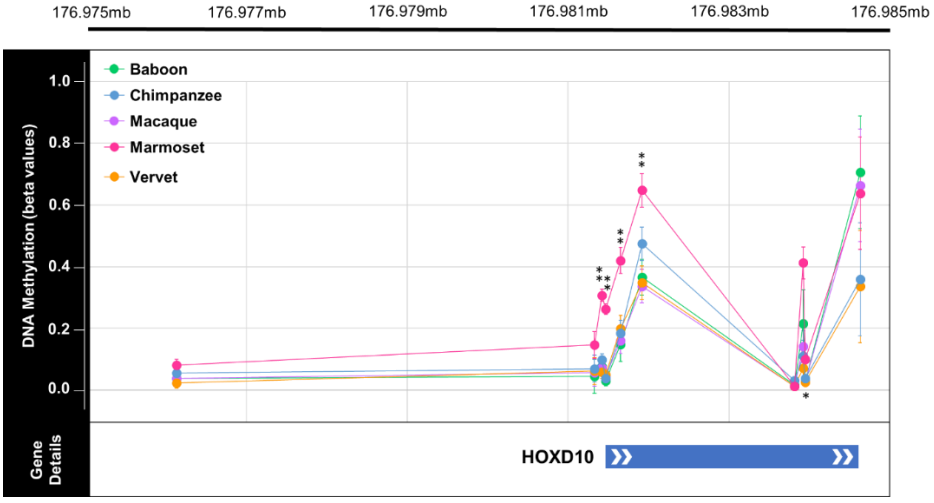

Figure 6.

Figure Legends:

Figure 1. Nonhuman Primate Sample Set Ages. Boxes represent one standard deviation from the average age, and whiskers depict the full range of ages for each species. Baboons (n=28) are 16.90±5.02 years, chimpanzees (n=4) are 11.31±1.87 years, macaques (n=10) are 14.75±2.65 years, marmosets (n=6) are 3.34±1.41 years, and vervets (n=10) are 9.31±10.30 years. Additional details can be found in Table S1.

Figure 2. Nonhuman Primate Morphological Measurements. See Table S6 for a detailed description of these measurements.

Figure 3. Methylation Levels at Species-Specific DMPs with Δβ≥0.4 Identified in the Inter-Specific Study. Heatmap depicting the DNA methylation levels (β values) of all species-specific DMPs with average absolute Δβ values greater than 0.4 between each taxonomic group (x-axis) in all nonhuman primate samples (n=58). The sex and age of each nonhuman primate are also provided (y-axis). Red indicates higher methylation at a DMP, while blue indicates lower methylation at a DMP. The dendrogram of all samples (y-axis) clusters individuals based on the similarity of their methylation patterns. Samples cluster based on species-level taxonomic groupings and as predicted based on known species phylogenetic histories.

Figure 4. Phylogeny Based on Average Species-Level Global Changes in Methylation. Observed phylogenetic relationship among nonhuman primates when considering average species-level global changes in methylation. This tree was constructed using the methylation levels for all finalized 39,802 filtered probes. I averaged the β values per probe within a species, used Euclidean distances to calculate the difference between every two species, and estimated a neighbor joining tree using this distance matrix. For the resulting tree, 1000 bootstraps were performed to determine confidence values for each branch. The number provide at each node indicates the number of bootstrap replicates that support it out of the 1000 performed.

Figure 5. Genome-Wide Methylation Levels Across *HOXD10* in Nonhuman Primates. Plot of the methylation levels of significant DMPs across the *HOXD10* gene (hg19 chr2:176981492-176984670). Plot shows the average β values for each DMP with error bars indicating 1 standard deviation in each direction for each comparative group (teal = baboon, orange = chimpanzee, purple = macaque, pink = marmoset, and light green = vervet). DMP chromosomal position in relation to the *HOXD10* gene is also depicted. This gene is of interest because it has been found to be differential methylation in ancient and modern hominin species (Gokhman et al. 2014). Of the sites depicted here, 5 DMPs were found to show significant species-specific methylation in marmosets. Of the 5 species-specific DMPs in the *HOXD10* gene of marmosets, 4 have Δβ between 0.2 and 0.3 (**) and 1 has a $\Delta\beta < 0.1$ (*). See Table S13 for additional information.

Figure 6. Gene-Specific Methylation Levels Across *HOXD10* in Nonhuman Primates. Bar plot of DNA methylation across the *HOXD10* gene (hg19 chr2:176981492-176984670), as well as upstream and downstream several hundred bases (hg19 chr2:176980532-176985117). Bars depict the presence (tall bar), partial presence (medium bar), or absence (low bar) of methylation at human derived CpG sites in 15 nonhuman primate samples – 3 baboons, 3 macaques, 3 vervets, 3 chimpanzees, and 3 marmosets. While regular sequencing was very successful, bisulfite sequencing was less successful, with several sequence reads uninterpretable. As such, nonhuman primate methylation data is only available for a subset of the CpGs known in humans. Partial presence of methylation was called when sequencing fluorescence peaks for cytosine and thymine were both present at a particular site and one was at least half the size of the other. Overall, these data provide additional information regarding gene-specific methylation levels across *HOXD10*. CpG sites that were also targeted by the EPIC array are highlighted in yellow and include cg18115040 (chr2, position 176981328), cg25371634 (chr2, position 176981422), cg13217260 (chr2, position 176981469), cg03918304 (chr2, position 176981654), cg17489939 (chr2, position 176981919), cg26708100 (chr2, position 176983815), cg10393811 (chr2, position 176983927), cg08992581 (chr2, position 176983949), and cg06005169 (chr2, position 176984634). See Table S18 and Files S8-S9 for additional information.